12

Antilock Braking Systems

Antilock braking systems (also known as antiskid braking systems) for vehicles are discussed here because they represent perhaps the most involved commonly used systems for automatic brake control. The data collection, analysis, and system design involved may suggest initial procedures to be followed for clutch and brake automation in other applications.

Design of an antilock system (ABS) for highway vehicles requires decisions to what is to be measured, how it is to be measured, and how to use the data to prevent skidding. These systems are different from the early antilock systems in that they are computer based, so they collect and process more data.

The first patent for antilock brakes was granted in Germany in 1905 [1], and the first antilock brakes for railroad cars were available in 1943 [2]. Electronic control of antilock brakes was widely incorporated into aircraft by 1960 [3] in order both to control aircraft skidding and to prevent excessive wear to the tires on the landing gear of large aircraft. Although it may be difficult to specify when the first extension to highway vehicles began, Ford and Kelsey Hayes produced an ABS system for the rear wheels only of the 1969 Thunderbird [4]. Introduction of what was said to be modern electronically controlled ABS for passenger cars was by Daimler-Benz [5] and BOSCH [6] in 1978.

Because of the proprietary nature of the available antiskid and traction control systems, the latter portion of this chapter, dealing with antiskid braking and traction control systems, will be a combination of information from the literature and of conjecture regarding the possible techniques available for achieving brake control.

I. TIRE/ROAD FRICTION COEFFICIENT

Antilock brake control for stopping a vehicle in what is intended to be a straight-line path clearly requires some method for detecting the skid, or slip, of each wheel, for assimilating the data from all wheels, for analyzing this data to estimate the vehicle's motion, and for selecting the appropriate commands to be sent to each wheel or set of wheels both to stop the vehicle and to maintain stability.

Figure 1(a) portrays the condition in which there is no slip between the wheel and the road. Under these conditions, a wheel of radius r rotating with angular velocity ω_0 about its axis of rotation (the centerline of the axle to which it is attached) at any instant also rotates about its instantaneous center (the idealized point where it contacts the road as though there were no tire

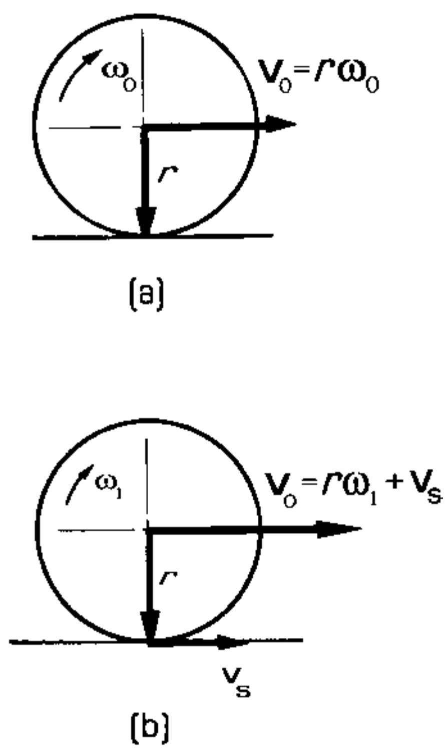

Figure 1 Velocity v_0 is the vehicle velocity as calculated (a) for a wheel rolling with angular velocity ω_0 without slip and (b) for rolling with angular velocity ω_1 and with slip velocity v_s.

deformation) with angular velocity ω_0. Hence, calculation of the rotation about the instantaneous center reveals that the axle moves horizontally with velocity v_0, as given by

$$v_0 = r\omega_0 \tag{1-1}$$

If there is slip between the wheel and the road, as in Figure 1(b), and if v_1 denotes the velocity of the axle with respect to the point where the wheel contacts the road, then the velocity of the axle relative to that point is given by

$$v_1 = r\omega_1 \tag{1-2}$$

where ω_1 is the angular velocity of the wheel about its axis of symmetry, which is perpendicular to the plane of the wheel. Thus, if the wheel slips with velocity

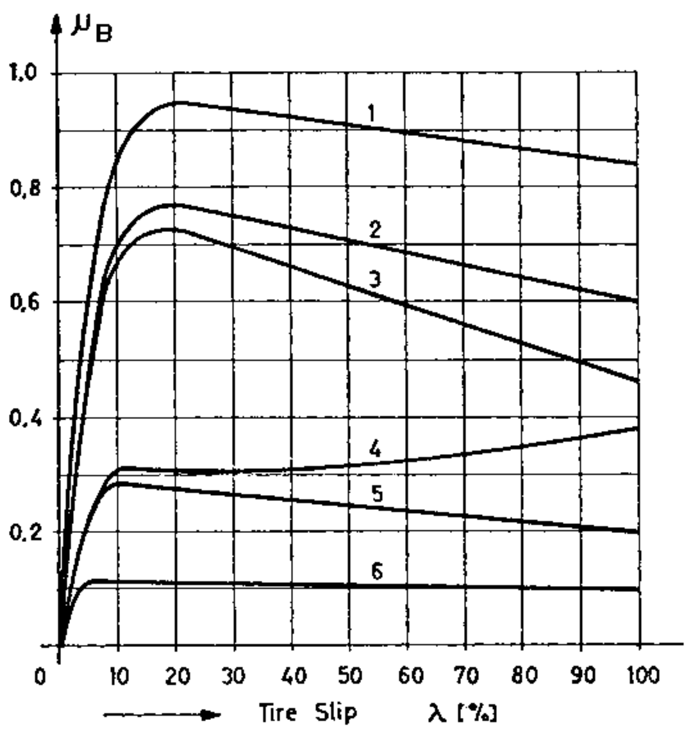

FIGURE 2 μ_B as a function of λ for (1) dry asphalt, (2) wet asphalt, thin water film, (3) wet asphalt, thick water film, (4) fresh snow, (5) packed snow, (6) glare ice. The positive slope of curve 4 with increasing λ is due to snow build-up in front of the tire as its rotation slows to zero.

v_s (i.e., the point where the wheel contacts the road moves with velocity v_s), then the velocity v_0 of the vehicle relative to the road is given by

$$v_0 = v_1 + v_s \tag{1-3}$$

Wheel slip during braking is commonly described by the slip ratio λ, as defined by

$$\lambda = \frac{v_s}{v_0} = \frac{v_0 - v_1}{v_0}. \tag{1-4}$$

The slip ratio is frequently presented as a percentage, $\lambda(\%) = 100\lambda$, as in Figure 2.

For reasons that may include tire flexibility, tension and torsion of the tread within the contact patch, and the continual replacement of material within the tire's contact patch, the complex nature of the tire's contact with the road within the contact patch means that the coefficient of friction, here represented by μ_B, does not immediately jump from its static to its dynamic value, as illustrated in Figure 2 [7]. That portion of each curve between $\lambda = 0$ and the maximum, except for curve 4, may be considered a stable region, in that initial braking causes the friction coefficient to increase so that increased brake pressure within this region is effective in reducing vehicle velocity. The region beyond the maximum in μ_B may be considered a region of instability, because, except for curve 4, increased brake pressure to further slow wheel rotation becomes increasingly ineffective in slowing the vehicle itself due to a decreasing friction coefficient. Returning to curve 4, its local maximum is also followed by a region of instability, but that region is followed by a stable region caused by the build up of snow in front of the wheel as its rotation slows.

II. MECHANICAL SKID DETECTION

Early antilock braking systems used annular disks that were friction driven to rotate with each wheel during normal acceleration and deceleration but that would slip as frictional resistance was overcome during abnormal or panic breaking, as a means of detecting wheel deceleration. Whenever the wheel would decelerate beyond a certain threshold, the disk that was concentric with it would continue rotating and thereby trip some mechanism that would reduce brake pressure. This technique, or a modification of it, was the only practical means of detecting wheel deceleration prior to the introduction of microprocessors. It was also relatively inexpensive and therefore its use continued through 1968, and perhaps beyone, for some inexpensive European automobiles. An example was the Lucas Girling Stop Control System (SCS), which is explained in the paragraphs below Figures 3–5, taken from Ref. 8, which describe the modulator. It was designed for front wheel drive (FWD) vehicles and employed only two modulators, one on each front wheel. Each modulator controlled its front wheel and the diagonally opposite rear wheel through a proportioning valve, as required by European regulations. Displayed components in these figures are

1. Drive shaft
2. Flywheel
3. Flywheel bearing
4. Ball and ramp drive
5. Clutch
6. Flywheel spring
7. Dump valve
8. Dump valve spring

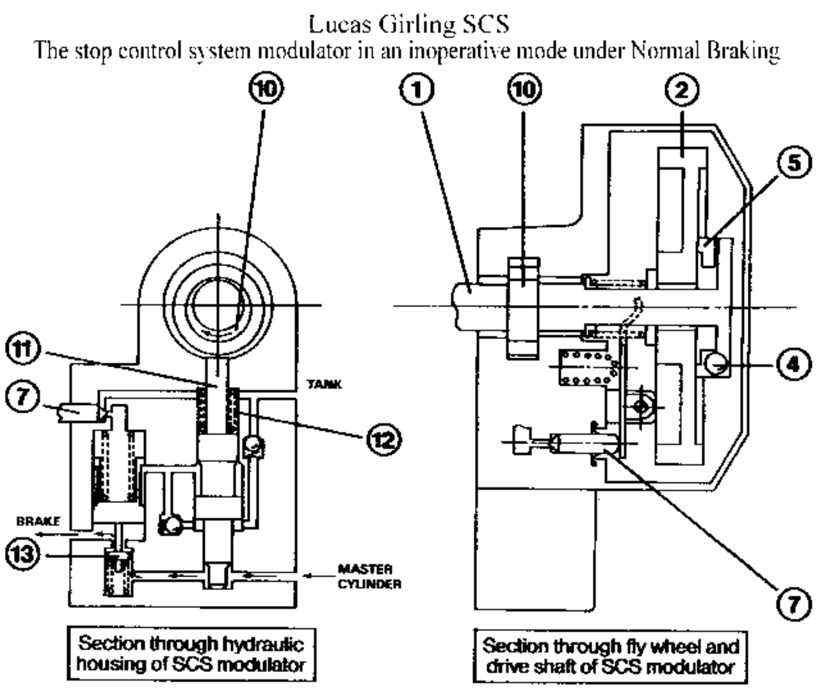

FIGURE 3 Flywheel and valve positions for the Lucas Girling SCS during normal braking.

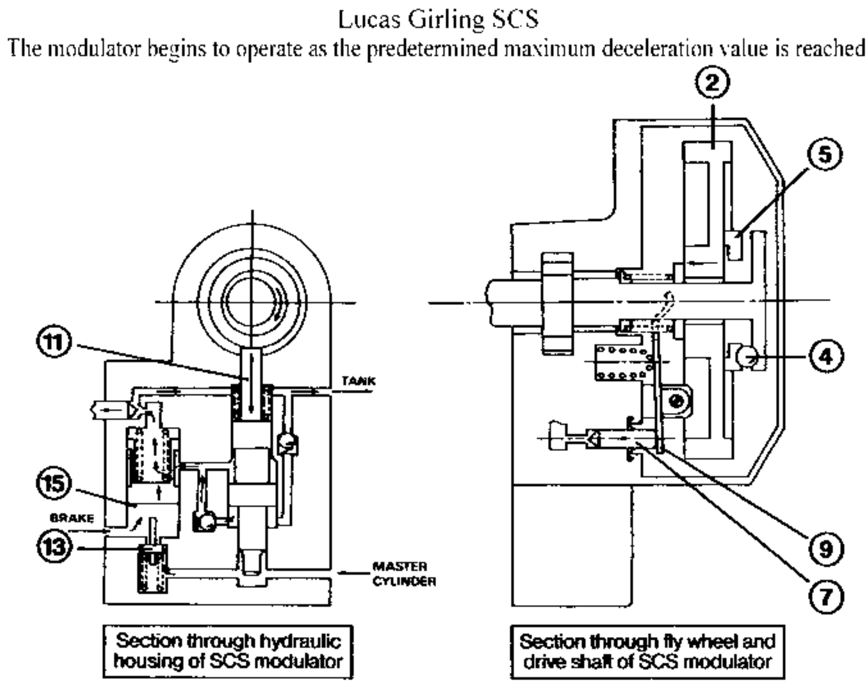

FIGURE 4 Flywheel and valve positions for the Lucas Girling SCS during panic braking.

9. Dump valve lever
10. Eccentric cam
11. Pump piston
12. Piston spring
13. Cutoff valve
14. Deboost piston spring
15. Deboost piston
16. Cutoff valve spring
17. Pump inlet valve
18. Pump outlet valve

Since the text below each figure was reproduced directly from Ref. 8. Figures 9 and 10 mentioned in Figure 4 correspond to Figures 3 and 5 as reproduced here.

All systems using rotating disks that must move axially to engage the brake control mechanism are handicapped by the time required to accelerate

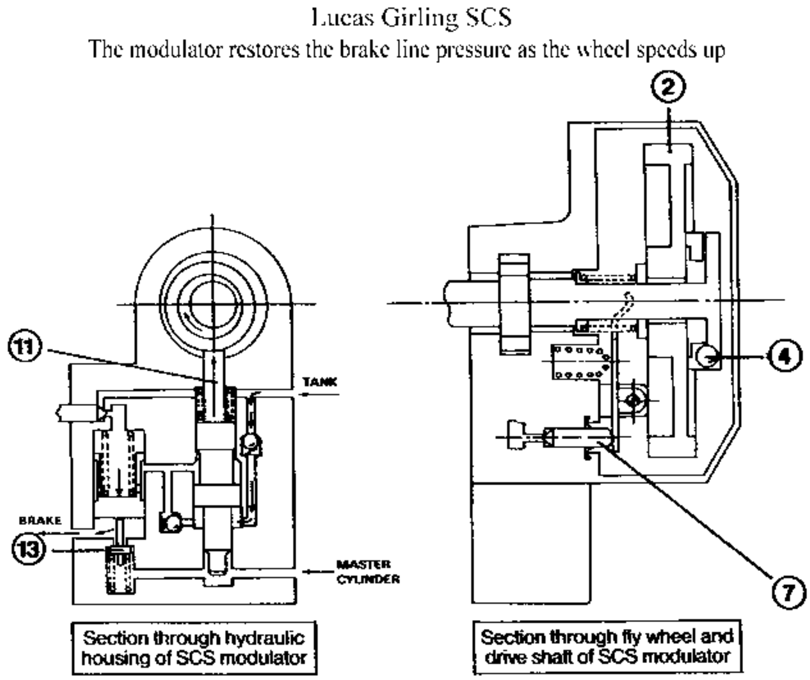

FIGURE 5 Flywheel and valve positions for the Lucas Girling SCS during return to normal braking.

the mass of the disk laterally over the required distance s. This relationship is qualitatively similar to that for the distance traveled by a mass m that is accelerated from rest by a force F over time t:

$$\frac{x}{s} = \frac{F}{2m}(x, y)^2 \qquad \text{(2-1)}$$

where x $(0 \leq x \leq s)$ is that portion of distance s traveled during time t $(0 \leq t \leq \tau)$, where t is the corresponding portion of the activation time t (see Figure 6). Thus, in the first half of the required time, the mass has moved only one-fourth of the required distance.

Faster response may be had by using electrical wheel-speed sensors that measure wheel speed and send that data to a small, dedicated computer known as an *electronic control unit*, or an ECU.

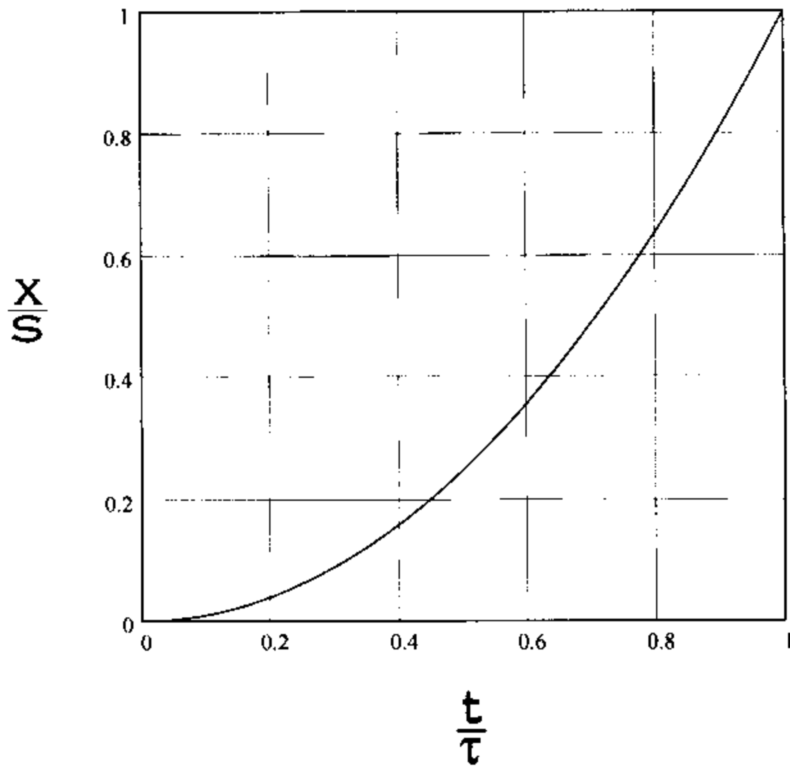

FIGURE 6 Graph of x/s as a function of t/τ from equation 12-1.

III. ELECTRICAL SKID DETECTION: SENSORS

Development of relatively inexpensive microprocessors, accelerometers, and electromagnetic wheel-speed sensors that could be incorporated into automotive controls permitted more precise measurement of wheel speed and, hence, vehicle speed, acceleration, and deceleration along with rapid detection of and improved response to individual wheel deceleration associated with wheel skid.

Addition of a small dedicated computer known as an electronic control unti, or an ECU, to an antilock system allows the correlation of data from wheel-speed sensors on each of all four wheels into a preprogrammed decision and control process. Presently each wheel-speed sensor consists of two components: a permanent bar magnet with a coil of wire wrapped around it and a sensor ring, as shown in Figure 7. The sensor ring rotates with the

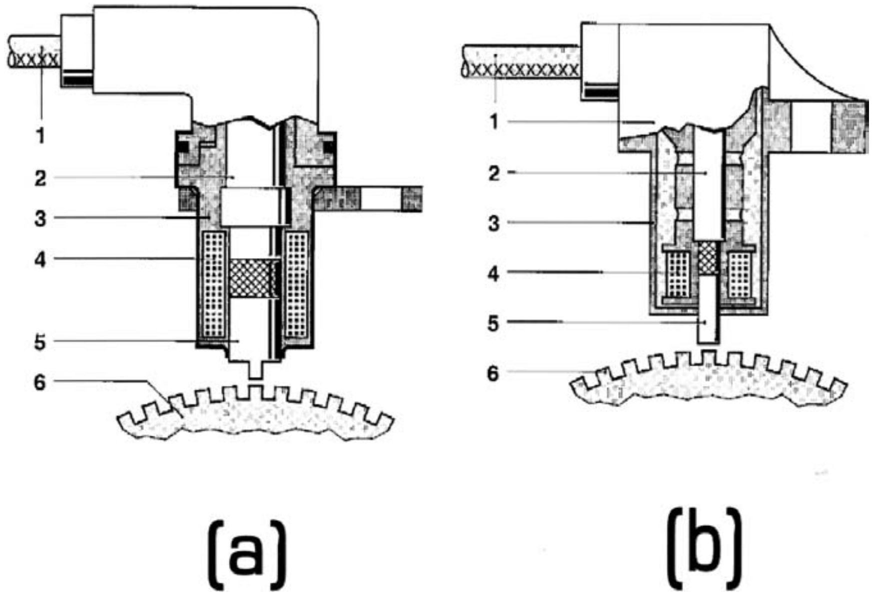

FIGURE 7 Sensor (a) has a chisel pole pin and sensor (b) has a cylindrical pole pin. The components in both: (1) electric cable, (2) permanent magnet, (3) housing, (4) winding, (5) pole pin, and (6) sensor ring. (Courtesy Robert Bosch GmbH, Stuttgart, Germany.)

vehicle wheel while the permanent magnet and its housing remain fixed relative to the vehicle's frame. As the wheel and the attached sensor ring rotate together, the magnetic field associated with the permanent magnet changes as a pole piece approaches and leaves each tooth on the toothed sensor ring. A fluctuating current is generated in the coil as the magnetic field fluctuates, with each fluctuation corresponding to the passage of a tooth.

These sensors also may be in the wheel bearings, in the differential, or on any other component whose rotation maintains a constant relationship to the wheel's rotation.

IV. ELECTRICAL SKID DETECTION: CONTROL

The ECU calculates wheel speed by counting the fluctuations per unit of time and differentiates the speed to calculate wheel acceleration or deceleration, wherein deceleration is handled as negative acceleration. In the absence of independent data on the motion of the vehicle itself, data from the wheel speed sensors must be used to estimate vehicle speed. When all wheels give the same vehicle speed, to within a specified error limit, that common speed is taken to be the vehicle speed. When all wheels do not give the same speed, wheel slip is assumed. The problem, of course, is to decide which wheel is slipping.

Typically the ECU in a front wheel drive vehicle with an antilock brake system will evaluate two data sets, one for the right front wheel and the left rear wheel and the other for the left front wheel and the right rear wheel. A typical rear wheel drive vehicle will also evaluate two data sets but one set will be for the front wheels and the other will be for the rear wheels. In either case, most systems test for wheel slip by compare diagonally opposed wheels in one of two ways: one is for the ECU control algorithm to use the signal from the faster of the two wheels as a reference speed for brake pressure modulation, known as the *select-high* method, the other is for the ECU to use the signal from the slower of the two wheels as the reference speed, known as the *select-low* method.

The proprietary control program, or algorithm, reacts once slip is detected. If the only input data is wheel speeds and their calculated acceleration/deceleration, the program may recall from permanent memory the greatest wheel acceleration/deceleration that is possible under zero-slip conditions. Hence, greater acceleration or greater deceleration (more negative acceleration) at a particular wheel indicates slip at that wheel.

Part of the ECU calculations is that of associating a wheel's rotational speed with the optimum wheel slip from equation (1-4) for λ between values λ_1 and λ_2, in which λ_1 may be 10% and λ_2 may be 20%, for example. This may be achieved by returning to equation (1-4) and solving for v_1 and then replacing v_1 and v_0 with the associated values of $r\omega_1$ and $r\omega_0$, respectively, where r is the wheel radius, to get

$$\omega_1 = \omega_0(1 - \lambda_1)$$

Likewise,

$$\omega_2 = \omega_0(1 - \lambda_2) \tag{4-1}$$

Since $\lambda_1 < \lambda_2$, it follows that $\omega_1 > \omega_2$ during braking. Thus, whenever the angular velocity ω of the wheel is such that it lies between ω_1 and ω_2, that is, whenever

$$\omega_1 \geq \omega \geq \omega_2$$

the slip velocity of the wheel is optimum, so the braking pressure will be held constant.

If $\omega \geq \omega_1$ (i.e., if the angular velocity of the wheel is large enough relative to ω_0 for the slip velocity to be small enough to lie between 0 and λ_1), the brake pressure may be increased because doing so will move the slip velocity into the optimum regions. If $\omega \leq \omega_2$ (i.e., if the angular velocity of the wheel is so small relative to ω_0 that the slip velocity is large), the brake pressure will be reduced in an attempt to move the slip velocity back to the optimum region.

Figure 8 represents most, if not all, ECUs that calculate angular acceleration from the measured wheel angular velocity in order to anticipate velocity changes in the next few milliseconds. This ability to anticipate velocity changes accounts for the superior performance of an electronically

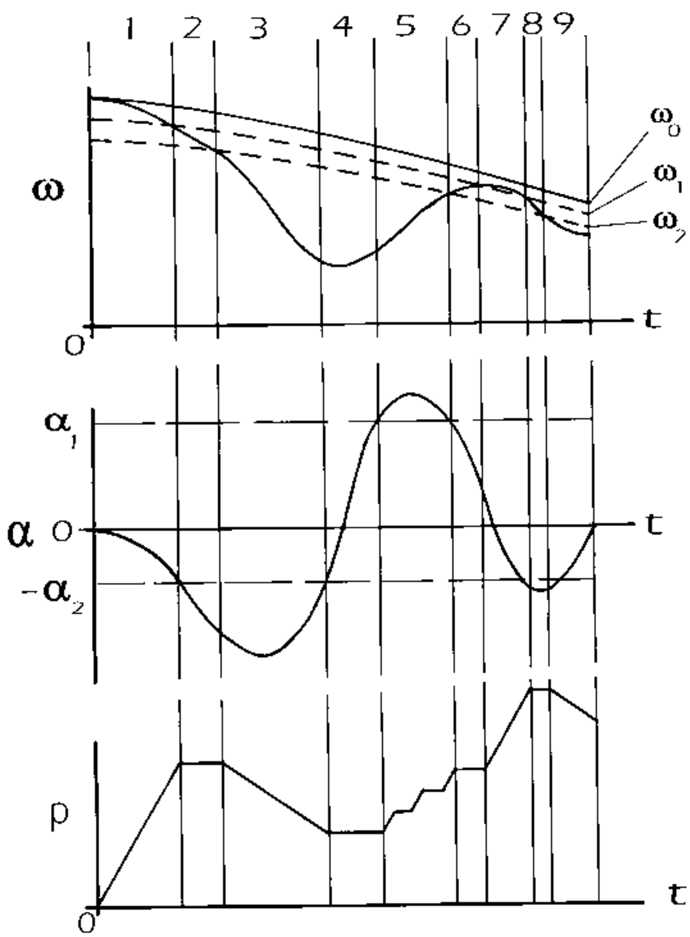

FIGURE 8 Estimated wheel reference angular velocity ω, optimum slip limits ω_1 and ω_2, angular acceleration α with decision limits α_1 and α_2, and brake pressure p, all as a function of time t.

controlled ABS over a less expensive one that relies upon a rotating annular ring to activate braking after velocity changes have begun.

An already noted, in an ABS that has no independent means of finding the vehicle velocity, the ECU memory in many such systems may contain typical data for the decrease in velocity as the brakes are applied for a selected road condition, as represented by the upper curve in Figure 2. The bottom graph in Figure 8 shows the pressure changes as commanded for a wheel by an ECU that does not alter the reference angular velocity ω_0 for zero slip while the ABS is in control of braking. The dashed lines labeled ω_1 and ω_2 bound the range of ω within which μ_B is at or near its maximum value.

ABS control is triggered by the wheel deceleration in region 1, which exceeds the reference deceleration α_2 (i.e., negative acceleration is less than-α_2) as it crosses into the optimum slip region, region 2, for braking where angular velocity ω is larger than ω_1 [9]. At this point the ECU calls for constant brake pressure until either the acceleration reverses or the angular velocity falls below ω_2, which is the case in this instance. Once ω is below ω_2 in region 3, the brake pressure is reduced until the acceleration increases enough to again be greater than$-\alpha_2$. In region 4, the brake pressure stays constant until the acceleration is larger than α_1, which indicates that the wheel is speeding up and wheel slip is being reduced to the point that it may again enter the optimum region. Thus the pressure is increased in region 5 in small steps, and the acceleration is checked after each step before commanding the next step. Wheel slip enters the optimum slip range in region 6, and brake pressure is again held constant. Once the wheel's angular velocity in region 7 rises above ω_1, it is in the stable region of Figure 6, and the brake pressure may be increased until the slip velocity enters the optimum range between ω_1 and ω_2 in region 8, where the ECU again holds the pressure constant. In region 9, ω is below ω_2, so brake pressure is reduced.

Similar logic holds in systems that employ accelerometer information to indicate actual vehicle response to the braking action of all wheels [10]. Since vehicle velocity and acceleration are determined independently from each wheel's angular velocity and angular acceleration, the road conditions at each wheel associated with the curves in Figure 2 may be estimated from calculations of μ_B and its gradients as a function of λ.

With this information, the reference curve for ω may be continuously updated to give better data on wheel slip, as displayed in Figure 9, which in turn should usually yield shorter stopping distances when used with equally well-programmed ECUs. As in Figure 8, the ω_0 curve represents the angular velocity of the particular wheel, which is directly related to the velocity of the vehicle when there is zero slip between the wheel and the road.

Again the ABS is activated at the beginning of region 1 when the acceleration falls below$-\alpha_2$, at which point the angular velocity ω exceeds ω_1

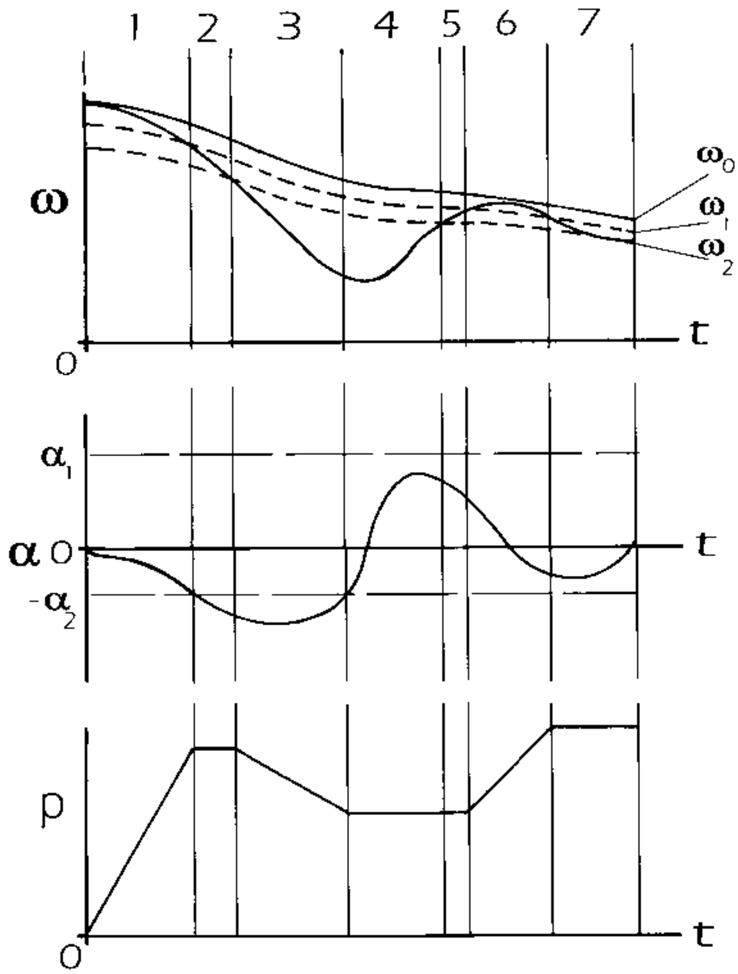

FIGURE 9 Wheel reference angular velocity ω based upon accelerator data, optimum slip limits ω_1 and ω_2, angular acceleration α with limits α_1 and α_2, and brake pressure *p*, all as a function of time *t*.

and the ECU holds the brake pressure constant throughout region 2. Because braking of all four wheels has caused the vehicle to slow, as detected by one or more accelerometers, the reference angular velocity has decreased in region 2 and continues to decrease in regions 3 and 4 due to the action of the remaining wheels, even though this wheel continues to slip. Brake pressure is reduced in region 3 because $\omega < \omega_2$ and $\alpha < -\alpha_2$. Brake pressure is held constant in region 4 because the acceleration is larger than $-\alpha_2$. It remains constant in region 5 because the velocity is between ω_1 and ω_2, and it increases in region 6 because the velocity has increased to a value greater than ω_1, which places it in the stable region where μ_B increases as the brake pressure increases. Finally, brake pressure remains constant through region 7 because ω has again moved into the optimum range.

Control systems described in Figures 8 and 9 are but two of many possible control methods. The system implied in Figure 8 may be improved by an ECU that remembers all of the road conditions shown in Figure 2 and compares all wheel velocities and accelerations to select the appropriate curve. For example, if all wheels decelerate quickly so that the negative angular acceleration falls below $-\alpha_2$ for all wheels, the ECU may assume the vehicle is on glare (black) ice, curve 6.

The decision process itself, as illustrated in Figures 8 and 9, is independent of whether or not that particular wheel is driven. Driven wheels have a larger effective moment of inertia than do undriven wheels, however, which will slow their response time to braking relative to an undriven wheel. Clearly their effective moment of inertia will depend upon what components are automatically disengaged during brake application. Some ECUs may be designed to account for this by receiving data that indicate when the wheels are engaged to a drive train.

Additional control may be had if an ECU has input from accelerometers, such as shown in Figure 10, that are positioned to measure both longitudinal and transverse acceleration. With both longitudinal and transverse accelerometer data, the ECU can compare accelerations to detect both spinning and transverse sliding during panic stops and other driving maneuvers and thereby can better maintain stability to the extent possible with brake control alone.

An example of the analysis associated with a particular accelerometer arrangement may be had by supposing that four accelerometers are arranged with their sensitive axes lying in a common horizontal plane that is parallel to the plane of motion of the vehicle. Also suppose that they are placed in the vehicle with two at the right front and two at the left front, each at distance R from an arbitrary reference point P in the plane, as shown in Figure 11. Accelerometers in each pair are positioned such that their sensitive axes are mutually perpendicular: One is parallel to the longitudinal axis of the vehicle, and the other is perpendicular to the longitudinal axis of the vehicle.

Let A and α denote the linear acceleration at point P and the angular acceleration about P, respectively, let a_{1L} and a_{1T} represent the accelerations measured in the longitudinal and transverse directions, respectively, at location 1, and let a_{2L} and a_{2T} represent the accelerations measured in the

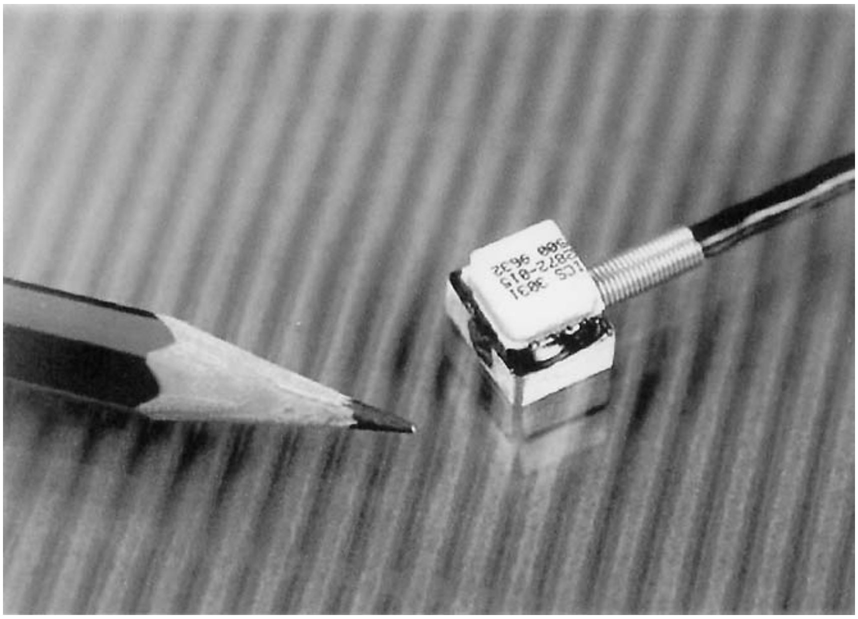

FIGURE 10 Single-axis accelerometer capable of measuring acceleration from $\pm 20g$ to $\pm 500g$, depending upon the model, which may be attached to the vehicle. (Courtesy GS Sensors, Ephrata, PA.)

longitudinal and transverse directions, in that order, at location 2. Let Ω denote the angular velocity of the spin of the vehicle about point P.

In terms of the dimensions shown in Figure 11, the accelerations measured by accelerometers a_{1L}, a_{1T}, a_{2L}, and a_{2T} are given by

$$a_{1L} = A \cos \theta + R\Omega^2 \cos \phi - R\alpha \sin \phi \quad (4\text{-}1)$$

$$a_{1T} = A \sin \theta + R\Omega^2 \sin \phi + R\alpha \cos \phi \quad (4\text{-}2)$$

$$a_{2L} = A \cos \theta + R\Omega^2 \cos \phi + R\alpha \sin \phi \quad (4\text{-}3)$$

$$a_{2T} = -A \sin \theta + R\Omega^2 \sin \theta - R\alpha \cos \phi \quad (4\text{-}4)$$

From the measured accelerations, the ECU can provide

$$\Omega = \sqrt{\frac{a_{1T} + a_{2T}}{2R \sin \phi}} \quad (4\text{-}5)$$

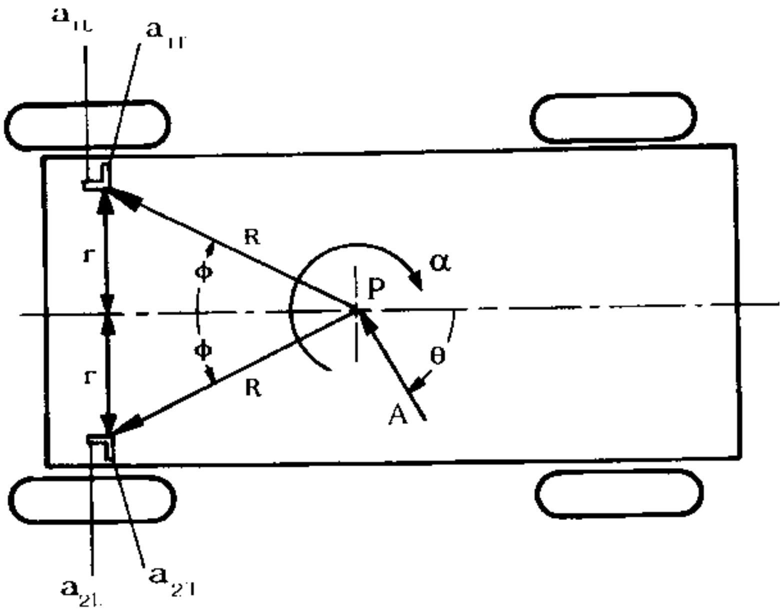

FIGURE 11 Plan view of accelerometer locations in a vehicle. Accelerometers a_{1L} and a_{2L} record positive in the forward direction (motion right to left); accelerometers a_{1T} and a_{2T} record positive outward (away from the centerline).

and

$$\alpha = \frac{a_{2L} - a_{1L}}{2\ R \cos \phi} \tag{4-6}$$

Note that angular velocity Ω was found without integration of the angular acceleration α with respect to time. However, because it appears in equations (4-1) through (4-4) as Ω^2, only its magnitude may be calculated. This is consistent with the centrifugal force being independent of the direction of rotation.

By defining B_1 and B_2 as

$$B_1 \frac{a_{1L} + a_{2L}}{2} - R\Omega^2 \cos \phi \tag{4-7}$$

$$B_2 = \frac{a_{1T} - a_{2T}}{2} - Ra \cos \phi \tag{4-8}$$

the acceleration A may be found from

$$A = \sqrt{B_1^2 + B_2^2} \tag{4-9}$$

and angle θ may be calculated from

$$\theta = a\tan\, 2(x, y)\frac{180}{\pi} \tag{4-10}$$

in which $a$tan 2 (x,y) calls a program that calculates θ from sin θ and cos θ and places the result in the proper quadrant in a coordinate system in which $\theta = 0$ on the positive x-axis and θ is positive in the counterclockwise direction. In equation (4-10),

$$x = a_{1L} + a_{2L} - 2R\Omega^2 \cos\,\phi \tag{4-11}$$

and

$$y = a_{1T} - a_{2T} - 2R\alpha \cos\,\phi \tag{4-12}$$

Finding the linear velocity of the vehicle does require integration. A simple means of numerical integration is for the ECU to remember the last calculated velocity v_{i-1} at time t_{i-1} and thereby calculate the latest velocity v_i at time t_i from

$$v_i = \frac{A_i + A_{i-1}}{2}\Delta_t + v_{i-1} \tag{4-11}$$

in terms of the time interval $\Delta t = t_i - t_{i\text{-}1}$ between accelerometer readings. An even simpler formula may be to replace the average acceleration over the sampling period $[(A_i + A_{i\text{-}1})/2]$ with the last measured acceleration A_i. This second choice emphasizes the last acceleration measurement and in some cases may be equally satisfactory as formula (4-11). Whether to use either of these formulas or another numerical formula depends upon the vehicle's inertia, braking response times, and perhaps other factors, such as the sampling time and the expected acceleration range, along with the expected accumulated error over the time that the ABS operates.

Depending upon the ECU program, control may be improved by merging this information with present data on the steering angles and angular rates of the front wheels. Similar data from all wheels may be used for vehicles in which all wheels steer.

Commands from the ECU are transmitted to the brakes through either hydraulic lines or electrical lines, which may differ in number from the data lines that run from the wheel sensors to the ECU. For example, in front wheel drive automobiles, all wheels are fitted with wheel sensors, but the ECU typically may have only two command lines, or circuits: One controls the right front and left rear wheels and the second controls the left front and right rear wheels. Rear wheel drive automobiles typically may have one command line to the front wheels and one to the rear wheels. Four-wheel-drive vehicles may have four control lines: one to each wheel. Data lines and control lines generally are more in number and the ECU programs are usually more elaborate for trucks and buses.

A system that includes the control both of braking and of acceleration during driving is commonly referred to as *fraction control system*, or TCS.

Although Figure 2 also may apply to vehicle acceleration, equation (1-4) must be modified to read

$$\lambda = \frac{v_1 - v_0}{v_0} = \frac{\omega_1 - \omega_0}{\omega_0} \tag{4-11}$$

if λ is to remain positive. Here v_1 represents the velocity the vehicle would have achieved during acceleration if there were no slip and v_0 represents the actual vehicle velocity. Associated wheel angular velocities are represented by ω_1 and ω_0.

For additional information on published details of ABS and TCS designs, see publications from the Society of Automotive Enginers (SAE), such as Ref. 11, from BOSCH publications, such as Ref. 9, and from other automotive engineering journals.

Example 1

To demonstrate that equation (4-5), (4-6), (4-9), and (4-10) yield the angular and linear accelerations and the magnitude of vehicle rotation, suppose that an accelerating vehicle's motion at a particular instant is equivalent to the center of gravity's accelerating at 14.9 ft/sec^2 at an angle of -8° relative to the vehicle centerline and to the vehicle rotating with an angular velocity of 1.9 rad/sec and an angular acceleration of -1.7 rad/sec^2 about its center of gravity. Let the center of gravity be such that $R = 3$ ft and $\varphi = 18^\circ$.

Substitution of $A = 14.9$, $R = 3$, $\Omega = 1.9$, $\varphi = 18^\circ$, and $\theta = -8^\circ$ into equations (4-1) through (4-4) yields

$$a_{1L} = 18.076 \text{ ft/sec}^2 \qquad a_{1T} = -13.574 \text{ ft/sec}^2$$

$$a_{2L} = 25.736 \text{ ft/sec}^2 \qquad a_{2T} = -2.692 \text{ ft/sec}^2$$

Substitution of these values into (4.5), (4-6), (4-9), and (4-10), yields

$$A = 14.9 \text{ ft/sec}^2 \quad \Omega = 1.9 \text{ rad/sec} \qquad \alpha = -1.7 \text{ rad/sec}^2$$

$$\theta = -8^\circ$$

Example 2

During braking, a vehicle decelerates with a motion that is equivalent to a linear deceleration of 20 m/sec^2 along a line oriented at 30° relative to the vehicular centerline, an angular acceleration of 11.7 rad/sec^2, and an angular velocity of −4.2 rad/sec. Accordingly, enter $A = -20$ m/sec^2, $R = 1$ m, $\Omega = -4.2$ m/sec, $\varphi = 18°$, and $\theta = 30°$ into equations (4-1) through (4-4). The result is

$$a_{1L} = -4.159 \text{ m/sec}^2 \qquad a_{2L} = 3.072 \text{ m/sec}^2$$
$$a_{1T} = 6.578 \text{ m/sec}^2 \qquad a_{2T} = 4.329 \text{ m/sec}^2$$

Substitution of these accelerations into equations (4.5), (4-6), (4-9), and (4-10), yields

$$A = 20 \text{ m/sec}^2 \qquad \Omega = 4.2 \text{ m/sec} \qquad \alpha = 11.7 \text{ rad/sec}^2$$
$$\theta = -150°$$

which indicates that the foregoing relations correctly evaluate the input data to describe the vehicle's motion except for the algebraic sign of Ω.

Accelerations and velocities used in our two examples are for demonstration only. Most ABS and TCS programs analyze and process input data rapidly enough that the controlled vehicle follows the driver's input commands (stopping, turning, accelerating, and backing) to the extent that deviations between the commands and the response of the vehicle are unnoticed under most conditions.

V. NOTATION

A, a	linear acceleration (l/t^2)
F	force (ml/t^2)
m	mass (m)
R, r	radius (l)
s	stopping distance (l)
t	time (t)
v	linear velocity (l/t)
x	distance (l)
α	angular acceleration ($1/t^2$)
λ	tire slip (1)
φ	angle (1)
θ	angle (1)
τ	stopping time (t)
Ω	angular velocity (t^{-1})
ω	angular velocity (t^{-1})

VI. FORMULA COLLECTION

Slip velocity, linear:

$$v_s = v_0 - v_1$$

Slip velocity, angular:

$$\omega_s = \omega_0 - \omega_s$$

Acceleration:

$$a_{1L} = A \cos\theta + R\Omega^2 \cos\varphi - R\alpha \sin\varphi$$
$$a_{1T} = A \sin\theta + R\Omega^2 \sin\varphi + R\alpha \cos\varphi$$
$$a_{2L} = A \cos\theta + R\Omega^2 \cos\varphi + R\alpha \sin\varphi$$
$$a_{2T} = -A \sin\theta + R\Omega^2 \sin\varphi - R\alpha \cos\varphi$$

Angular velocity:

$$\Omega = \sqrt{\frac{a_{1T} + a_{2T}}{2R \sin\phi}}$$

Angular acceleration:

$$\alpha = \frac{a_{2L} - a_{1L}}{2R \sin\phi}$$

Linear acceleration:

$$A = \sqrt{B_1^2 + B_2^2}$$

Linear velocity:

$$v_i = \frac{A_i + A_{i-1}}{2}\Delta t + v_{i-1}$$

REFERENCES

1. Lieber, H., Czinczel, A. (1987). Antiskid System for Passenger Cars with a Digital Electronic Control Unit. In: Martin, J. M., Gritt, P.S., eds. *Anti-Lock Braking Systems for Passenger Cars and Light Trucks-A Review*. Warrendale, PA: Society of Automotive Engineers, pp. 233–239.
2. Buckman, L. C. (1998). *Commercial Vehicle Braking Systems: Air Brakes, ABS and Beyond*. Warrendale, PA: Society of Automotive Engineers.
3. (1987). Martin, J. M., Gritt, P. S., eds. Preface, *Anti-Lock Braking Systems for Passenger Cars and Light Trucks—A Review*. Warrendale, PA: Society of Automotive Engineers.
4. Douglas, J. W., Schafer, T. C. (1987). The Chrysler "Sure-Brake"—The first Production Four-Wheel Anti-Skid System. In: Martin, J. M., Gritt, P. S., eds. *Anti-Lock Braking Systems for Passenger Cars and Light Trucks—A Review*. Warrendale, PA: Society of Automotive Engineers.
5. Burckhardt, M. (1979). Erfahrungen bei der Konzeption und Entwicklung des Mercedes-Benz/Bosch-Anti-Blockier-Systems (ABS) ATZ, 81:5.

6. Lieber, H. (1979). Antiblockiersystems für Personenwagen mit digitaler Elek tronik-Aufbau und Funktion, ATZ, 81:11.
7. Müller, P., Czinczel, A. (1987). Electronic Anti-Skid System—Performance and Application. In: Martin, J. M., Gritt, P. S., eds. *Anti-Lock Braking Systems for Passenger Cars and Light Trucks—A Review*. Warrendale, PA: Society of Auto motive Engineers, pp. 25–33.
8. Newton, W.R., Riddy, F.T. (1987). Evaluation Criteria for Low-Cost Anti-Lock Brake Systems for FWD Passenger Cars. In: Martin, J. M., Gritt, P. S., eds. *Anti-Lock Braking Systems for Passenger Cars and Light Trucks-A Review*. Warrendale, PA: Society of Automotive Engineers, pp. 277–287.
9. (1994). Bauer, H., ed. *Brake System for Passenger Cars*. Trans. P. Girling, Robert Bosch GmbH.
10. Yoneda, S., Naitoh, Y., Kigoshi, H. (1987). Rear Bruke Lock-Up Control System of Mitsubishi Starlou. In: Martin, J. M., Gritt, P. S., eds. *Anti-Lock Braking Systems for Passenger Cars and Light Trucks—A Review*. Warrendale, PA: Society of Automotive Engineers, pp. 249–255.
11. Schwarz, R., Willimowski, M., Isermann, R., Willimowski, P. (1997). In: *Overview of ABS/TCS and Brake Technology*. Warrendale, PA: Society of Automotive Engineers, pp. 123–133.